Molecular Catalysis 601 (2026) 116139

Contents lists available at ScienceDirect

Molecular Catalysis

journal homepage: www.journals.elsevier.com/molecular-catalysis

Research Paper

Amine substitution pattern governs catalytic performance in manganese-PNN ketone hydrogenation

Zsófia Császár [a], Márta Nagy [a], Ágnes Gömöry [b], Margit Kovács [c], Attila C. Bényei [d], József Bakos [a], Gergely Farkas [a,*]

[a] University of Pannonia, Research Group of Organic Chemistry – Synthesis and Catalysis, Egyetem u. 10, H-8200 Veszprém, Hungary
[b] MS Proteomics Research Group, HUN-REN Research Centre for Natural Sciences, Magyar Tudósok körútja 2, Budapest H-1117, Hungary
[c] NMR Laboratory, University of Pannonia, Egyetem u. 10, H-8200 Veszprém, Hungary
[d] University of Debrecen, Department of Physical Chemistry, Egyetem tér 1, H-4032 Debrecen, Hungary

ARTICLE INFO

Keywords:
Homogeneous catalysis
Manganese pincer complexes
Metal-ligand cooperation
Structure-activity relationship
Ligand design

ABSTRACT

A highly modular synthetic strategy based on the ring opening of propane-1,3-diol cyclic sulfate by the corresponding diamines enabled the straightforward preparation of potentially tridentate phosphine-diamine (PNN) ligands of the general formula $Ph_2P(CH_2)_3N(R^1)(CH_2)_2NR^2R^3$ (R^1, R^2, R^3 = H or CH_3), featuring amine functionalities with different substitution patterns. Using these novel ligands, manganese(I) complexes of the type $[Mn(PNN)(CO)_2Br]$, incorporating the catalytically critical NH subunits in distinct chemical environments, were synthesized and evaluated in the hydrogenation of various ketones under different reaction conditions. Catalysts containing a terminal NH_2 unit exhibited significantly higher activity than those bearing $NHCH_3$ or $N(CH_3)_2$ moieties. Despite the expected reduction in ligand-metal cooperativity upon N-methylation, the presence of an internal N-methyl group in addition to the terminal amino functionality further enhanced catalytic performance. Density functional theory (DFT) calculations revealed substantial differences in the coordination stereochemistry of the PNN ligands within the catalytically active manganese hydride complexes, which correlate with the observed reactivity trends. The most active catalyst displayed exceptionally high turnover number among PNN-containing manganese complexes in ketone hydrogenation.

1. Introduction

Catalytic hydrogenation of polar double bonds (eg. C═O or C═N) constitutes one of the cornerstone transformations in homogeneous catalysis, underpinning numerous processes in fine chemical synthesis, pharmaceutical manufacturing and materials chemistry [1–4]. Traditionally, this transformation has been dominated by noble-metal catalysts based on ruthenium, rhodium, iridium, and palladium, which combine high activity with excellent selectivity and stability [5]. However, increasing economic and sustainability concerns associated with the limited availability, high cost, and environmental footprint of these precious metals have driven intense research efforts toward the development of catalysts based on earth-abundant 3d transition metals such as iron, cobalt, nickel, and manganese [6]. Among these, manganese has emerged as a particularly attractive alternative because of its low toxicity, high natural abundance, easy availability and outstanding stability under catalytic conditions [7,8]. Additionally, Mn(I)-complexes with pincer-type frameworks have demonstrated remarkable activity in hydrogenation and dehydrogenation reactions, [9,10] including the reduction of aldehydes, [11,12] ketones, [11,13–18] esters, [19–22] amides, [23–25] imides, [26] nitriles, [11,27,28] heterocycles [29–31] and CO_2-derived substrates [32–34]. A defining feature of many of these systems is the presence of metal-ligand cooperation, [35,36] typically involving a nitrogen-containing site that participates directly in activation of molecular H_2 (or hydrogen donor molecule) and also facilitates the hydride transfer from the metal. In other words, the metal center and the ligand directly cooperate in both the bond-breaking and bond-forming steps of the catalytic cycle. This concept, pioneered in noble-metal catalysis, [37–39] has proven equally powerful for manganese, [40] enabling catalytic cycles that avoid high oxidation-state intermediates and instead rely on bifunctional reactivity at the metal-ligand interface. Despite these advances, subtle variations in ligand structure – such as backbone flexibility, [30,41–43] hemilabile nature [28,44–46] or donor stereoelectronic properties [43,47–49] –

* Corresponding author.
E-mail address: farkas.gergely@mk.uni-pannon.hu (G. Farkas).

https://doi.org/10.1016/j.mcat.2026.116139
Received 20 April 2026; Received in revised form 28 May 2026; Accepted 10 June 2026
Available online 26 June 2026

often lead to dramatic changes in catalytic performance, underscoring the need for new systematic ligand design strategies (Fig. 1).

PNN and PNP ligands represent a particularly useful platform within this context. The combination of phosphorus and nitrogen donors creates a tunable balance between electronic donation, steric protection, and cooperative functionality. However, compared with their PNP counterparts, alkane-diyl based PNN ligands also offer themselves to structural modification with respect to systematic modulation of the amine substitution pattern. Despite the well-recognized importance of NH functionality in cooperative ligand design, the systematic variation of the donoratom substitution pattern in a diamine moiety remains scarce, [50] and, to the best of our knowledge, there is no example for such studies in Mn-PNN systems. Moreover, synthetic access to such tailored ligands is often non-trivial, further limiting the scope of the available structure-activity relationship studies in this research area.

Within this framework, the present study introduces a family of highly modular PNN ligands of the general formula $Ph_2P(CH_2)_3N(R^1)(CH_2)_2NR^2R^3$, featuring systematically varied amine substitution pattern (Fig. 1). The ligand architecture enables precise positioning of N—H or N—Me functionalities (R, R' and R'' = H or Me) within the same framework, allowing direct assessment of how local chemical environment influences manganese coordination behavior and catalytic performance. Importantly, the synthetic strategy employed allows rapid access to these ligands in a straightforward and scalable manner, making them attractive for broader catalyst development efforts.

2. Results and discussions

2.1. Synthesis of the ligands

The novel ligands **L1-L4** were synthesized in two straightforward steps starting from the cyclic sulfate of propane-1,3-diol (Scheme 1). First, nucleophilic ring opening of the sulfate with the corresponding diamine was performed, followed by the reaction of the resulting sulfated amine with lithium diphenylphosphide. This sequence afforded the desired ligands in moderate to good yields. Compound **L5** was prepared in a subsequent methylation step of **L4** by the Eschweiler-Clarke reaction [51]. The new PNN type compounds share the same alkane-diyl-based C3-C2 type framework but possess different N-substitution patterns.

2.2. Synthesis of manganese complexes [Mn(L)(CO)$_2$Br] (Mn1-Mn5)

The treatment of $[Mn(CO)_5Br]$ with one molar equivalent of ligands **L1**-**L5** in toluene at 90 °C for 3 h afforded the desired manganese complexes [Mn(**L**)$(CO)_2$Br] (**Mn1**-**Mn5**) as yellow-orange solids in high yields (Scheme 2). Over the course of the reaction **Mn1** and **Mn2** precipitated out from solution, while **Mn3-Mn5** proved to be more soluble in toluene. The complexes were characterized by IR and NMR spectroscopy, high resolution mass spectrometry (HRMS), and one structure could be resolved by X-ray crystallography.

The solution and solid phase infrared (IR) spectra of **Mn1-Mn5** display two strong CO bands of similar intensity. Based on the comparison with the IR spectra of known Mn(I)-carbonyl complexes, [20,41,52,53] *mer*-[Mn(PNN)$(CO)_2$Br] configuration could be suggested for **Mn1-Mn5**.

The NMR spectra of the complexes were recorded either in CD_2Cl_2 or in benzene-d_6, depending on solubility. Although in benzene-d_6 somewhat narrower signals could be observed, the poor solubility of **Mn1-Mn3** in benzene prompted us to investigate their spectrum in CD_2Cl_2. (In fact, the solubility of **Mn1** proved to be rather limited even in dichloromethane.) The coordination of the PNN ligands as tridentate systems were confirmed by the significant coordination shifts of their ^{31}P and corresponding ^{1}H NMR signals. Complexes **Mn2-Mn5** exhibited one broad signal in the ^{31}P NMR spectra in the range of 64.2–73.81 ppm, indicating the formation of a single diastereomer [54]. In contrast to that, in the rather dilute solution of **Mn1** in CD_2Cl_2 three ^{31}P NMR signals appeared at 89.36, 70.75 and 64.20 ppm in a ratio of 5, 77 and 18%, respectively. To gain deeper insight into the solution phase behavior of complexes **Mn1-Mn5** we performed density functional theory optimizations (DFT) using the CAM-B3LYP functional combination with the SDD basis set and pseudopotential for Mn as well as the 6–31G* basis set for the rest of the atoms. The structures were optimized in the corresponding solvent using the CPCM implicit solvation model. All the possible combinations concerning the configuration of the central manganese atom and the stereogenic nitrogen donor(s) as well as the *fac-mer* arrangement of the PNN ligand were screened in the octahedral complexes. The calculations were consistent with the spectroscopic observations and for complexes **Mn2-Mn5** only one isomer proved to be more stable (with at least 7.1 kJ/mol lower in energy) compared to the others suggesting their formation in a stereoselective manner. For **Mn1**, however, geometry optimizations suggested the presence of three low energy species with relative enthalpies 0, 0.9 and 1 kJ/mol, that are either differing in the relative position of the internal N—H and the Mn-Br or related as *fac-mer* isomers (see the Supporting information).

It is proposed that, in addition to steric factors, the formation of an intramolecular NH…Br hydrogen bond can strongly contribute to the stabilization of specific spatial arrangements of the PNN ligand around the metal center. The presence of NH…X (X = Cl, Br) interactions in transition metal complexes is well precedented in the literature [55–59].

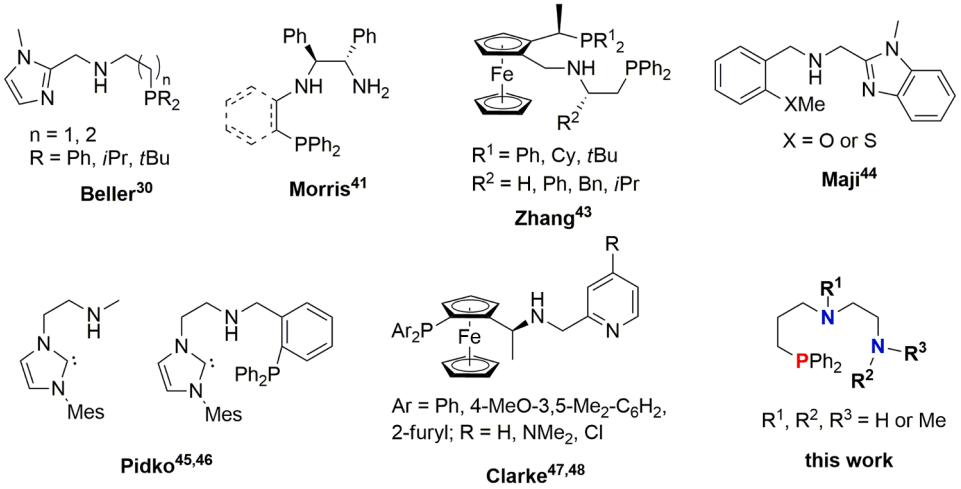

Fig. 1. Selected examples for the structural modifications of tridentate ligands used in manganese catalyzed hydrogenation.

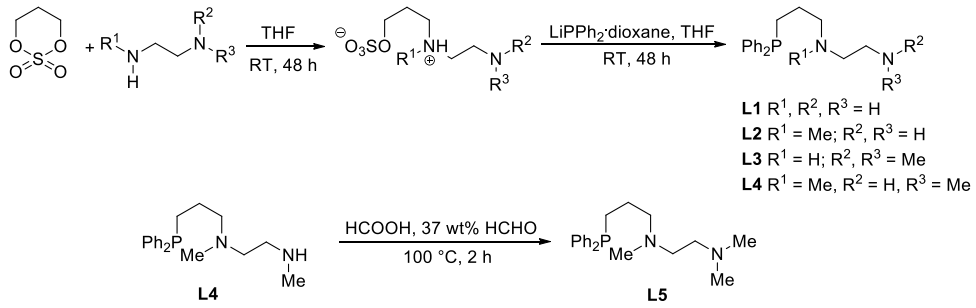

Scheme 1. Synthesis of PNN ligands **L1-L5**.

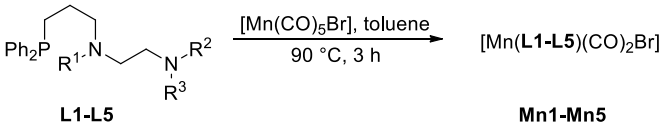

Scheme 2. Synthesis of complexes **Mn1-Mn5**.

In this context, it is not surprising that **Mn1**, containing an internal NH and a terminal NH_2 unit, can be stabilized in three low-energy isomers in which the N–H and Mn–Br units are arranged nearly parallel to each other (H–N–Mn–Br < 13°), thereby enabling the formation of an NH…Br hydrogen bond. Most importantly, the three most stable isomers of **Mn2** adopt the same configuration as the lowest-energy structures of **Mn1**; however, their relative enthalpies are 0, 17, and 17 kJ/mol, respectively. In the latter two structures, no N–H and Mn–Br bonds are aligned parallel to each other (H–N–Mn–Br > 38°). Similarly, the most stable diastereomer of **Mn3** and **Mn4** (having hydrogen bonds) are noticeably lower in energy (ΔH > 7 kJ/mol) than the next energetically most favorable structure without parallel N–H and Mn–Br units. Although **Mn5** lacks a suitable N–H bond for an NH…Br intramolecular interaction, steric factors appear to govern the stereoselective formation of the complex in this case.

In addition to spectroscopic investigations and theoretical calculations, a single crystal, suitable for X-ray structure determination, could be grown by the slow evaporation of the solvent from the solution of **Mn2** in dichloromethane. The X-ray structure supports, in all respects, the conclusions drawn from the IR and NMR analysis and the DFT calculations (Fig. 2). In the slightly distorted octahedral complex, the PNN ligand coordinates in a *meridional* fashion to the manganese center and the two carbonyl ligands are arranged in *cis* position relative to each other. The bromine ligand is directed *trans* to the Me substituent of the internal nitrogen donor. The six-membered ring formed by the P-N unit of the ligand adopts a chair conformation while the five-membered cycle is stabilized in *skew* arrangement. The NH…Br distance (2.723 Å) is considerably shorter than the expected van der Waals separation (3.05 Å) suggesting the presence of an intramolecular NH…Br hydrogen bond [60].

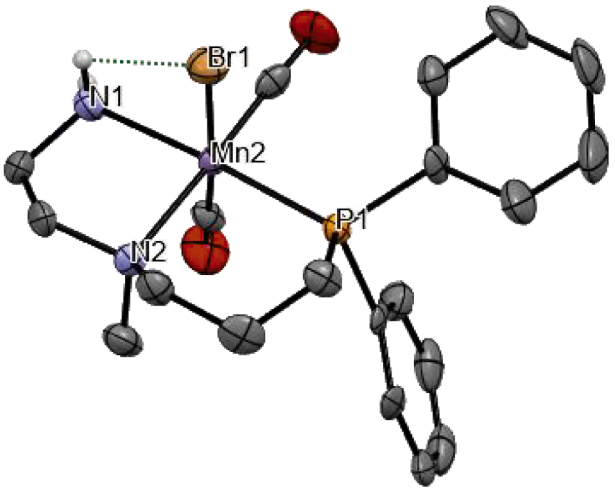

Fig. 2. ORTEP view of the molecular structure of complex **Mn2**, with thermal ellipsoids drawn at 50% probability level. Hydrogen atoms are omitted for clarity.

2.3. Catalytic studies

Ketone hydrogenation serves as an ideal benchmark reaction for evaluating new manganese catalysts. It is mechanistically well understood, experimentally convenient, and highly sensitive to catalyst design. Moreover, high turnover frequencies under mild conditions are essential for practical applications, particularly when targeting replacement of noble metal containing systems. Although several manganese pincer complexes have achieved impressive activities, further improvements are needed to fully match or surpass the performance of well-established ruthenium catalysts, especially at low catalyst loadings and under industrially relevant conditions.

Therefore, with complexes **Mn1-Mn5** in hand we set out to investigate their catalytic performance in the hydrogenation of acetophenone as substrate (Table 1). Initially, the catalysts were screened at 50 °C and 70 bar hydrogen pressure using ethanol as solvent and *t*BuOK as base. After 1 h reaction time it was clearly visible that catalyst with terminal NH_2 moiety (**Mn1** and **Mn2**, entries 1 and 3) outperform those without primary amino site (**Mn3-Mn5**, entries 5, 7 and 9). Importantly, **Mn2** provided the product with 79% conversion at a substrate/catalyst molar ratio of 500 (entry 3), while **Mn5** without N—H unit proved to be inactive under these conditions (entry 9). The catalytic reactions were also performed at 20 h reaction time to screen the stability of the catalysts. Similarly, **Mn1** and **Mn2** gave the best performance during prolonged reaction time resulting in the hydrogenation of the substrate with complete conversion (entries 2 and 4). Catalyst **Mn3** afforded the product with 51% conversion, while 9% conversion could be achieved using **Mn4** as catalyst. This trend further highlights the importance of primary terminal amino functionality for satisfactory catalytic performance. No catalytic activity could be observed in the lack of PNN ligand (entry 11), using $[Mn(CO)_5Br]$ solely as catalyst.

The very low catalytic activity achieved by complex **Mn5** highlights the fact that the presence of NH units is necessary to achieve noticeable catalytic activity. It is therefore reasonable to assume that the catalytic reaction follows the well-known outer sphere mechanism, [10] where the NH moiety of the precatalyst is deprotonated in the presence of the base, resulting in the formation of an amido complex as catalytically active species in the activation of molecular H_2 via metal-ligand cooperation (MLC). After H_2 addition, the resulting hydrido-complexes containing Mn-H and N—H units serve as active hydrogenating agents: when the Mn-H and N—H bonds point in the same direction, an NH…O

Table 1
Hydrogenation of acetophenone: screening of catalysts Mn1-Mn5[a].

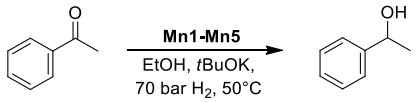

Entry	Catalyst	Ligand	Reaction time [h]	Conv. [%]
1	Mn1	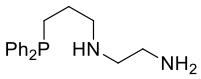	1	10
2			20	>99
3	Mn2	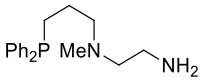	1	79
4			20	>99
5	Mn3	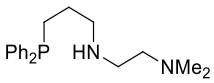	1	2
6			20	51
7	Mn4	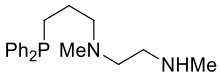	1	2
8			20	9
9	Mn5	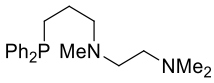	1	0
10			20	7
11	$[Mn(CO)_5Br]$	-	20	0

[a] Reaction conditions: catalyst: 0.006 mmol, *t*BuOK: 0.03 mmol, EtOH: 0.8 mL, acetophenone: 3 mmol, temperature: 50 °C, H_2 pressure: 70 bar. Conversion was determined by GC.

hydrogen bond forms and the substrate is positioned perpendicularly to the H-Mn-N-H plane so that the carbonyl carbon is oriented above the Mn-H bond facilitating the hydride transfer from the catalysts to the substrate. Based on this, the relative position of the Mn-H and N—H bonds has crucial importance in catalytic activity. Indeed, only those complexes with their Mn-H *cis* to the N—H are believed to have reactivity according to the MLC mechanism [61–63]. Considering these facts, we modelled all the possible hydrido-complexes (**MnH1-MnH4**) formed from **Mn1-Mn4** using the same theoretical method outlined above to investigate their coordination chemistry affecting the relative position of their N—H unit.

The hydrido-Mn(PNN) complexes exhibit coordination stereochemistry markedly different from those of the bromo complexes **Mn1-Mn4** (Fig. 3). For **MnH1** and **MnH2** bearing PNN ligands with terminal NH_2 group, the lowest-energy species adopt a *fac* coordination mode (*fac*-**MnH1** and *fac*-**MnH2**, Fig. 3), in contrast to bromo-complexes **Mn1** and **Mn2**, where the PNN ligand has a *mer*-arrangement in the lowest energy isomer (for **Mn2** see Fig. 2). The enthalpy differences between the most stable and second most stable hydrido-Mn isomers are 8 and 6 kJ mol^{-1} for **MnH1** and **MnH2**, respectively. The most stable isomers are *fac*-**MnH1** and *fac*-**MnH2**, while the second most stable ones are *mer-cis*-**MnH1** and *mer-trans*-**MnH2**. In these *fac*- and *mer*-isomers, the Mn-H

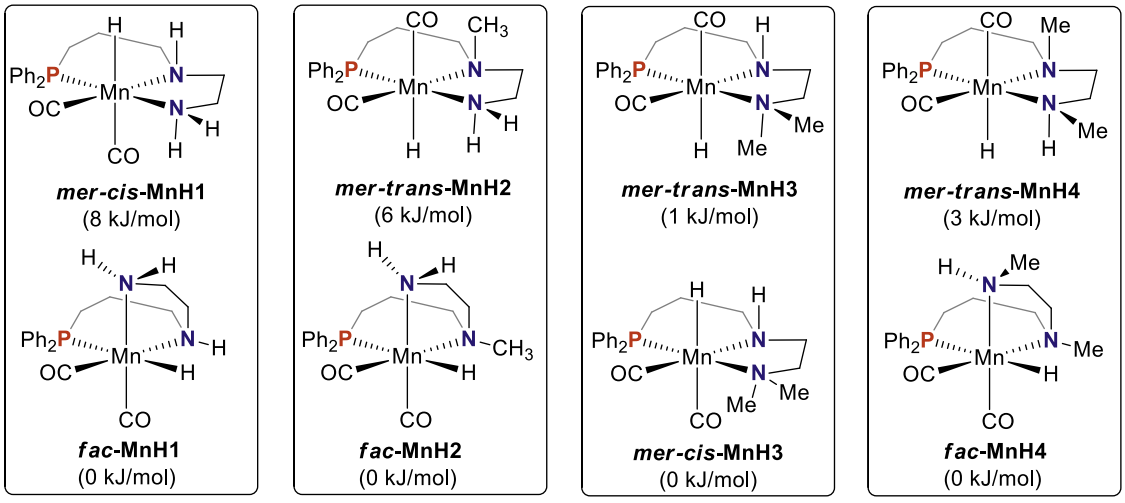

Fig. 3. The most stable geometries and calculated relative enthalpies of manganese-hydride complexes containing ligands **L1**-**L4** (*fac/mer* descriptors refer to the relative position of the PNN donoratoms, *cis/trans* descriptors define the position of the Mn-H relative to the internal N-R (R = Me or H) in the *mer* isomers).

unit is positioned *cis* to at least one N—H group (H-N-Mn-H dihedral angle $\leq 38°$) and is therefore expected to be accessible for efficient hydride transfer [64]. According to DFT calculations, **MnH3** exists as a mixture of two nearly isoenergetic isomers (*mer-trans*-**MnH3** and *mer-cis*-**MnH3**, $\Delta H \sim 1$ kJ mol^{-1}), both retaining the *mer* configuration of the parent **Mn3** complex. These isomers differ in the relative orientation of the N—H and Mn-H moieties, exhibiting *cis/trans* isomerism. Accordingly, only one of them is expected to be catalytically active. **MnH4** is also stabilized as two low-energy *fac/mer* isomers (*fac*-**MnH4** and *mer-trans*-**MnH4)**, with the *fac* arrangement being 3 kJ mol^{-1} lower in energy. However, in this *fac* isomer the terminal N—H and the Mn-H units are oriented in opposite directions, thus only the *mer* isomer is expected to be catalytically active, as in this structure the two hydrogen atoms are aligned parallel to each other.

Although no definitive conclusions can yet be drawn regarding the differences in catalytic activity among the systems modified with ligands **L1-L4**, several trends emerge from the combined theoretical and experimental results. First, *fac*-coordination of the PNN ligands becomes more favorable in the hydrido-complexes compared to the corresponding bromo-derivatives. Second, increasing the steric demand of the terminal amino moiety (NH_2 < NHMe < NMe_2) destabilizes the *fac*-isomers relative to the *mer*-assemblies of the hydrido–Mn complexes, most likely due to steric effects. These observations indicate that even subtle structural modifications can induce pronounced changes in the coordination stereochemistry of the catalytically active hydrido-species. Third, ligand modification also governs the accessibility of the catalytically favorable parallel Mn–H/N–H arrangement. Indeed, DFT calculations indicate that the most active Mn catalysts bearing ligands **L1** and **L2** form hydrido complexes in which the Mn–H and N–H bonds are oriented in the same direction, thereby enabling an efficient MLC pathway. In contrast, theoretical studies suggest that **L3** and **L4** do not coordinate stereoselectively to the metal center in **MnH3** and **MnH4**, respectively, both of which exhibit lower catalytic activity. In these cases, the Mn hydride complexes exist as mixtures of isomers, although only one diastereomer is competent for efficient hydride transfer according to the mechanistic rationale outlined above. A thermodynamically stable and catalytically inactive hydrido isomer featuring an antiparallel Mn–H/N–H arrangement may therefore represent an off-cycle species, leading to diminished catalytic turnover [41,65].

This DFT-based model is consistent with experimental observations and suggests that differences in coordination stereochemistry arising from distinct substitution patterns can strongly influence catalytic performance. It is evident, however, that structural parameters beyond the coordination differences between the hydrido complexes also exert a substantial influence on catalytic activity. Differences in the structure of the amido-Mn intermediates and the variations in the rate of H_2 activation, the equilibria between different isomers, or the electronic disparities among the ligand N-donor atoms may all play important roles. In addition, the possible involvement of further low-lying off-cycle intermediates (e.g., solvated species), whose stability may strongly depend on the PNN framework, could further contribute to the observed activity trends.

A rigorous and quantitative rationalization of the activity differences among **Mn1-Mn4** would, in principle, require a comprehensive computational investigation of the entire catalytic cycle, including the identification of transition states and the evaluation of multiple, potentially competing reaction pathways, equilibria and off-cycle processes. Given the structural flexibility of the PNN framework and the diversity of accessible coordination modes, several energetically similar reaction channels may coexist, leading to mechanistic scenarios of substantial complexity. In this context, the present study focuses on the relative stability and structural characteristics of the accessible hydrido isomers, which represent one important class of catalytically relevant intermediates. Although this approach does not provide a complete quantitative description of the catalytic cycle, it captures key structural parameters that directly influence hydride transfer and represents an important addition to the key structure-activity correlations consistent with the experimentally observed trends.

Nevertheless, systematic variation of the N-substitution pattern enables substantial enhancement of catalytic activity, underscoring the effectiveness of this strategy in catalyst design.

In the next set of experiments, we aimed to optimize the reaction conditions for the hydrogenation of acetophenone using **Mn2** as the catalyst (Table 2) and to explore the limits of the catalytic system. Increasing either the hydrogen pressure or the reaction temperature significantly improved the conversion (entries 1–4). In addition, when

Table 2
Optimization of reaction conditions in the hydrogenation of acetophenone using Mn2 as catalyst[a].

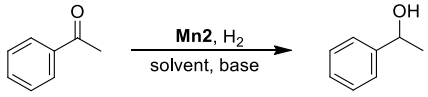

Entry	p(H_2) [bar]	T [°C]	Solvent	Base	B/C ratio	S/C ratio	Reaction time [h]	Conv. [%]
1	70	25	EtOH	*t*BuOK	5	500	1	16
2	50	50	EtOH	*t*BuOK	5	500	1	45
3	30	50	EtOH	*t*BuOK	5	500	1	25
4	30	80	EtOH	*t*BuOK	5	500	1	62
5	50	50	MeOH	*t*BuOK	5	500	1	>99
6	30	50	MeOH	*t*BuOK	5	500	1	65
7	50	50	*i*PrOH	*t*BuOK	5	500	1	7
8	50	50	MeOH	K_2CO_3	5	500	1	26
9	30	50	MeOH	KOH	5	500	1	62
10	30	50	MeOH	NaOMe	5	500	1	76
11[b]	30	50	MeOH	NaOMe	5	1 000	1	18
12[b]	30	50	MeOH	NaOMe	20	1 000	1	49
13[b]	30	50	MeOH	NaOMe	30	1 000	1	60
14[b]	30	50	MeOH	NaOMe	30	1 000	3	85
15[b]	30	50	MeOH	NaOMe	30	1 000	6	>99
16[c]	-	50	MeOH	NaOMe	30	1 000	1	0
17[d]	50	50	MeOH	NaOMe	30	10 000	24	97
18[e]	50	50	MeOH	NaOMe	30	20 000	48	71

[a] Reaction conditions: catalyst: 0.006 mmol of **Mn2**, solvent: 0.8 mL, acetophenone: 3 mmol. Conversion was determined by GC. [b]Catalyst: 0.003 mmol of **Mn2**, acetophenone: 3 mmol. [c]Catalyst: 0.003 mmol of **Mn2**, acetophenone: 3 mmol. No hydrogen was used. [d]Catalyst: 0.003 mmol of **Mn2**, acetophenone: 30 mmol, solvent: 3 mL. [e]Catalyst: 0.003 mmol of **Mn2**, acetophenone: 60 mmol, solvent: 4 mL.

Table 3
Hydrogenation of different ketones using Mn2 as catalyst[a].

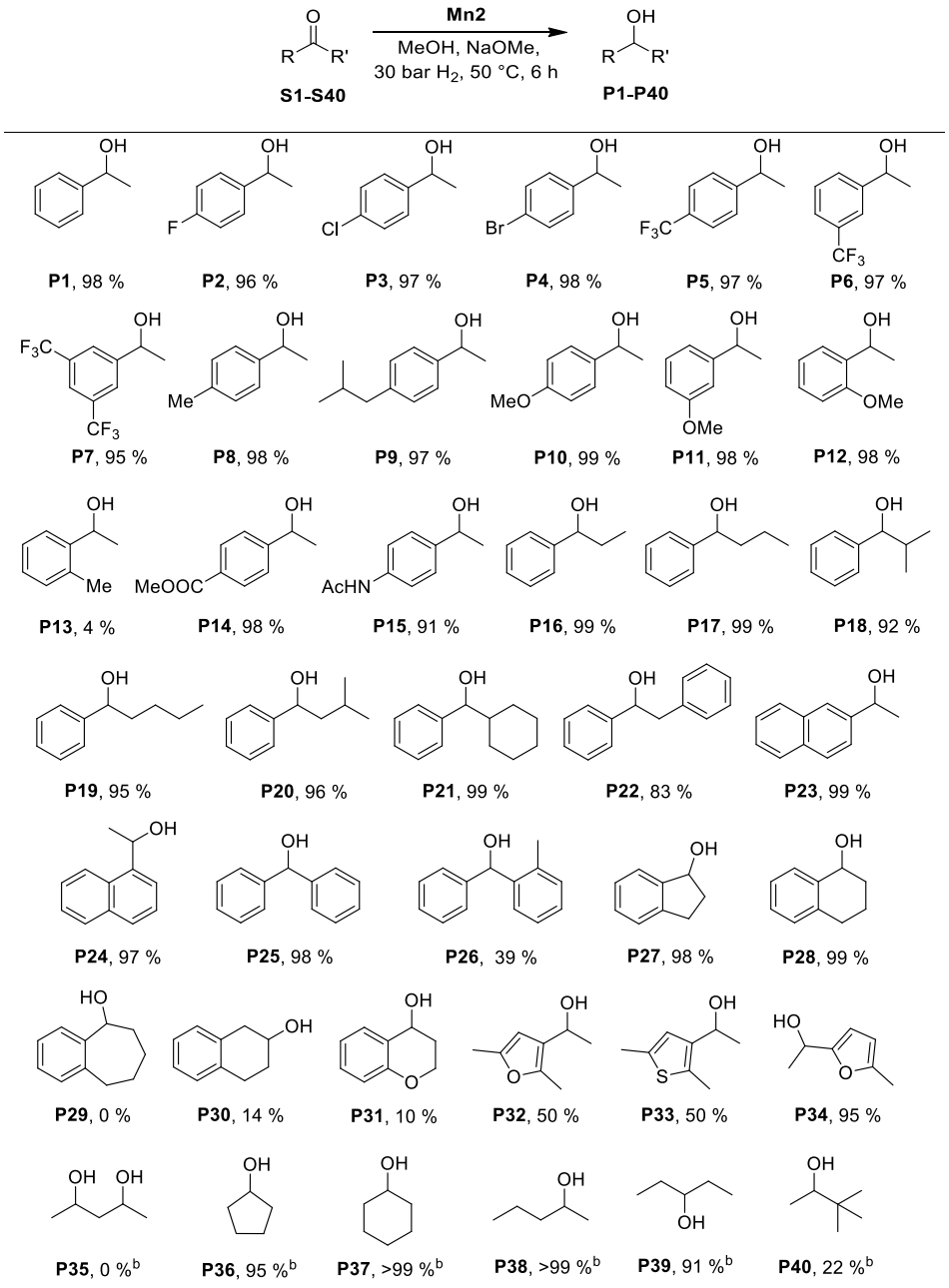

[a] Reaction conditions: catalyst: 0.003 mmol of **Mn2**, NaOMe: 0.09 mmol, substrate: 3 mmol, MeOH: 0.8 mL, temperature: 50 °C, H_2 pressure: 30 bar, reaction time: 6 h. The % values are isolated yields. [b]Conversion instead of isolated yield due to the volatility of the product. Conversion was determined by GC.

methanol was used as the solvent instead of the less polar ethanol or isopropanol, complete conversion of the substrate was achieved after 1 h at 50 °C under 50 bar of hydrogen pressure (entry 5).

Variation of the base (entries 8–10) revealed that the highest activity can be obtained in the presence of sodium methoxide (NaOMe). Increasing the molar ratio of this base relative to the catalyst from 5 to 30 resulted in complete conversion of the starting material at 50 °C under 30 bar H_2 with a substrate-to-catalyst ratio of 1000 (entry 15). To minimize the environmental impact of the reaction, the amount of base was not increased further. No conversion was observed in the lack of molecular hydrogen (entry 16).

In order to investigate the stability of the catalyst, additional experiments were performed at higher substrate-to-catalyst ratios under 50 bar H_2 at 50 °C. At an S/C ratio of 10 000, 97% conversion was achieved after 24 h (entry 17). Additionally, the catalytic reaction carried out at an S/C ratio of 20 000 and a reduced solvent volume resulted in a 71% conversion of the substrate, corresponding to a turnover number (TON) of 14 200 (entry 18). To the best of our knowledge this is one of the highest turnover numbers in homogeneous manganese-catalyzed ketone hydrogenation reported to date [15,47,66,67].

Finally, we investigated the substrate tolerance of the catalytic system to prove the synthetic utility of this non-noble metal-based methodology. A broad range of ketonic substrates were subjected to hydrogenation at an S/C ratio of 1000 under 50 bar pressure and at 50

°C temperature using **Mn2** as catalyst (Table 3). Simple alkyl-aryl ketones with alkyl-, alkoxy- or halogen-containing substituents in *meta*- or *para*-position (**S2**-**S11**) could easily be hydrogenated under optimized conditions regardless of electronic nature of the substituent. Interestingly, the reduction of *o*-methyl-acetophenone (**S13**) proved to be quite slow, even though its *o*-methoxy analogue (**S12**) could be hydrogenated smoothly under identical conditions. According to these observations, steric effects play an important role in determining the rate of hydrogenation. The catalyst tolerates well the modification of the structure of the alkyl-chain in alkyl-aryl ketones as products **P16**-**P22** could be isolated in high yields. Benzophenones **S25** and **S26** were hydrogenated to afford the corresponding benzhydrols; however, the more sterically hindered **P26** was obtained in lower yield. The reactivity of fused ring aromatic ketones **S27**-**S30** showed a pronounced dependency on the size of the aliphatic ring and the position of the carbonyl group. The seven-membered ring containing benzosuberone (**S29**) proved to be unreactive, and the hydrogenation of β-tetralone (**S30**) provided the alcohol **P30** with low isolated yield (14%). The hydrogenation of heterocyclic ketones **S31**-**S33** gave the corresponding alcohols with relatively low yields that can be attributed to their more pronounced steric demand. Contrarily, the transformation of heterocyclic ketone **S34** with less steric bulk led to the production of alcohol **P34** with high yield. Although pentane-2,4-dion (**S35**) proved to be unreactive under catalytic conditions, simple cyclic or acyclic dialkyl ketones **S36**-**S39** could smoothly be hydrogenated. Again, the substrates (e.g. **P40**) with sterically demanding alkyl groups could be converted to the desired alcohols with considerably lower yield.

3. Conclusions

In summary, the present work introduces a versatile ligand platform that enables systematic investigation of amine substitution effects in PNN-type manganese catalysts. The newly developed PNN ligands display markedly different coordination behavior in their manganese hydride complexes according to DFT calculations, with coordination preferences strongly influenced by the amine substitution pattern. Manganese complexes bearing ligands with terminal NH_2 units (**Mn1** and **Mn2**) exhibited superior catalytic performance compared to their analogues with more steric bulk at the terminal amin site (**Mn3**-**Mn5**). The highest activity was observed for **Mn2**, which contains tertiary internal and primary terminal amino functionality, enabling the efficient hydrogenation of aromatic, aliphatic, and heterocyclic ketones. Furthermore, the results demonstrate record-level catalytic performance for ketone hydrogenation within this ligand class, reaching a TON of 14 200 in the hydrogenation of acetophenone. We believe these findings advance both the fundamental understanding and the practical development of manganese-based hydrogenation catalysts, further highlighting the potential of earth-abundant metals in sustainable homogeneous catalysis.

CRediT authorship contribution statement

Zsófia Császár: Writing – review & editing, Supervision, Methodology, Investigation. **Márta Nagy:** Investigation. **Ágnes Gömöry:** Writing – review & editing, Investigation. **Margit Kovács:** Writing – review & editing, Investigation. **Attila C. Bényei:** Writing – review & editing, Investigation. **József Bakos:** Writing – review & editing. **Gergely Farkas:** Writing – review & editing, Writing – original draft, Supervision, Conceptualization.

Declaration of competing interest

The authors declare that they have no known competing financial interests or personal relationships that could have appeared to influence the work reported in this paper.

Acknowledgements

G. F. acknowledges support from the János Bolyai Research Scholarship of the Hungarian Academy of Sciences. The authors also gratefully acknowledge financial support provided by the project RRF-2.3.1–21–2022–00009 (National Laboratory for Renewable Energy) and by the TKP2021-NKTA-21 project.

Supplementary materials

Supplementary material associated with this article can be found, in the online version, at doi:10.1016/j.mcat.2026.116139.

Data availability

Data will be made available on request.

References

[1] A. Corma, S. Iborra, A. Velty, Chemical routes for the transformation of biomass into chemicals, Chem. Rev. 107 (2007) 2411–2502, https://doi.org/10.1021/cr050989d.
[2] S. Hashemzadeh, M.R. Rahimpour, Hydrogenation of ketones by homogeneous catalysts in, Eds.0, in: M.R. Rahimpour, M.A. Makarem, T. Roostaie, M. Meshksar (Eds.), Advances in Green and Sustainable Chemistry, Homogeneous Hydrogenation and Metathesis Reactions, Advances in Green and Sustainable Chemistry, Homogeneous Hydrogenation and Metathesis Reactions, 5, Elsevier, 2025, https://doi.org/10.1016/B978-0-443-15656-4.00004-5.
[3] K.C. Tan, T. He, Y.S. Chua, P. Chen, Recent advances of catalysis in the hydrogenation and dehydrogenation of N-heterocycles for hydrogen storage, J. Phys. Chem. C 125 (2021) 18553–18566, https://doi.org/10.1021/acs.jpcc.1c04783.
[4] X. Lan, T. Wang, Highly selective catalysts for the hydrogenation of unsaturated aldehydes: a review, ACS Catal. 10 (2020) 2764–2790, https://doi.org/10.1021/acscatal.9b04331.
[5] M.L. Clarke, G.J. Roff, Homogeneous hydrogenation of aldehydes, ketones, imines and carboxylic acid derivatives: chemoselectivity and catalytic activity, Eds, in: J. G. de Vries, C.J. Elsevier (Eds.), The Handbook of Homogeneous Hydrogenation, The Handbook of Homogeneous Hydrogenation, 1, Wiley-VCH, Weinheim, Germany, 2007, pp. 413–454, https://doi.org/10.1002/9783527619382.ch15.
[6] L. Alig, M. Fritz, S. Schneider, First-row transition metal (De)hydrogenation catalysis based on functional pincer ligands, Chem. Rev. 119 (2019) 2681–2751, https://doi.org/10.1021/acs.chemrev.8b00555.
[7] Jean-Baptiste Sortais, Manganese Catalysis in Organic Chemistry, Ed, Wiley-VCH, Weinheim, Germany, 2022, https://doi.org/10.1002/9783527826131.
[8] Y. Wang, M. Wang, Y. Li, Q. Liu, Homogeneous manganese-catalyzed hydrogenation and dehydrogenation reactions, Chemistry 7 (2021) 1180–1223, https://doi.org/10.1016/j.chempr.2020.11.013.
[9] M. Garbe, K. Junge, M. Beller, Homogeneous catalysis by Manganese-based pincer complexes, Eur. J. Org. Chem. 2017 (2017) 4344–4362, https://doi.org/10.1002/ejoc.201700376.
[10] P. Schlichter, C. Werlé, The rise of Manganese-catalyzed reduction reactions, Synthesis (Mass) 54 (2022) 517–534, https://doi.org/10.1055/a-1657-2634.
[11] S. Elangovan, C. Topf, S. Fischer, H. Jiao, A. Spannenberg, W. Baumann, R. Ludwig, K. Junge, M. Beller, Selective catalytic hydrogenations of nitriles, ketones, and aldehydes by well-defined manganese pincer complexes, J. Am. Chem. Soc. 138 (2016) 8809–8814, https://doi.org/10.1021/jacs.6b03709.
[12] M. Glatz, B. Stöger, D. Himmelbauer, L.F. Veiros, K. Kirchner, Chemoselective hydrogenation of aldehydes under mild, base-free conditions: manganese outperforms rhenium, ACS Catal 8 (2018) 4009–4016, https://doi.org/10.1021/acscatal.8b00153.
[13] F. Kallmeier, T. Irrgang, T. Dietel, R. Kempe, Highly active and selective manganese C=O bond hydrogenation catalysts: the importance of the multidentate ligand, the ancillary ligands, and the oxidation state, Angew. Chem. Int. Ed. 55 (2016) 11806–11809, https://doi.org/10.1002/anie.201606218.
[14] N.F. Both, J. Fessler, A. Vicenzi, K. Andres, A. Spannenberg, K. Junge, M. Beller, Air-stable manganese *NNS* pincer complexes enable ketone reduction at room temperature, ChemCatChem 16 (2024) e202301562, https://doi.org/10.1002/cctc.202301562.
[15] J. Yang, L. Yao, S. Liu, P. Gao, M. Han, Q. Liu, G.A. Solan, W.H. Sun, Manganese(I)-catalyzed asymmetric (transfer) hydrogenation of ketones: an insight into the effect of chiral PNN and NN ligands, J. Catal. 418 (2023) 40–50, https://doi.org/10.1016/j.jcat.2023.01.006.
[16] S. Zhang, Z. Ma, Y. Li, Y. Su, N. Ma, X. Guo, L. Li, Q. Liu, Z. Wang, Enhancing enantioselectivity of manganese catalyst for asymmetric transfer hydrogenation of ketones through *P,N,N*-chelation of a cyclooctyl pyridine, J. Catal. 437 (2024) 115682, https://doi.org/10.1016/j.jcat.2024.115682.
[17] Y. Su, Z. Ma, J. Wang, L. Li, X. Yan, N. Ma, Q. Liu, G.A. Solan, Z. Wang, Asymmetric transfer hydrogenation of ketones improved by PNN–Manganese complexes, J. Org. Chem. 89 (2024) 12318–12325, https://doi.org/10.1021/acs.joc.4c01253.

[18] Z. Wang, Y. Wang, Q. Lyu, D. Zhu, Z. Ma, B. Gansukh, L. Li, H. Liu, N. Ma, Z. Wang, The importance of alkali cations in manganese catalyzed asymmetric transfer hydrogenation of ketones: an insigth into the effect of „NH" and „C=N" groups in ligands, J. Catal. 444 (2025) 115998, https://doi.org/10.1016/j.jcat.2025.115998.

[19] S. Elangovan, M. Garbe, H. Jiao, A. Spannenberg, K. Junge, M. Beller, Hydrogenation of esters to alcohols catalyzed by defined manganese pincer complexes, Angew. Chem. Int. Ed. 55 (2016) 15364–15368.

[20] N.A. Espinosa-Jalapa, A. Nerush, L.J.W. Shimon, G. Leitus, L. Avram, Y. Ben-David, D. Milstein, Manganese-catalyzed hydrogenation of esters to alcohols, Chem. Eur. J. 23 (2017) 5934–5938, https://doi.org/10.1002/chem.201604991.

[21] M.B. Widegren, G.J. Harkness, A.M.Z. Slawin, D.B. Cordes, M.L. Clarke, A highly active manganese catalyst for enantioselective ketone and ester hydrogenation, Angew. Chem. Int. Ed. 56 (2017) 5825–5828, https://doi.org/10.1002/anie.201702406.

[22] Y. Su, Z. Ma, P. Han, X. Ren, N. Ma, Q. Liu, Q. Cao, Z. Wang, Suitable alkali cations improved Mn(I)-catalyzed hydrogenation of esters: an insight into the effect of bases and ligands' ring sizes on catalytic performance, J. Catal. 452 (2025) 116436, https://doi.org/10.1016/j.jcat.2025.116436.

[23] V. Papa, J.R. Cabrero-Antonino, E. Alberico, A. Spanneberg, K. Junge, H. Junge, M. Beller, Efficient and selective hydrogenation of amides to alcohols and amines using a well-defined manganese-PNN pincer complex Chem, Science 8 (2017) 3576–3585, https://doi.org/10.1039/C7SC00138J.

[24] J. Luk, C.L. Oates, J.A.F. Garcia, M.L. Clarke, A. Kumar, Manganese-catalyzed hydrogenation of amides and polyurethanes: is catalyst inhibition an additional barrier to the efficient hydrogenation of amides and their derivatives? Organometallics 43 (2024) 85–93, https://doi.org/10.1021/acs.organomet.3c00399.

[25] Y.-Q. Zou, S. Chakraborty, A. Nerush, D. Oren, Y. Diskin-Posner, Y. Ben-David, D. Milstein, Highly selective, Efficient deoxygenative hydrogenation of amides catalyzed by a Manganese Pincer complex via metal-ligand cooperation, ACS Catal. 8 (2018) 8014–8019, https://doi.org/10.1021/acscatal.8b02902.

[26] U.K. Das, T. Janes, A. Kumar, D. Milstein, Manganese catalyzed selective hydrogenation of cyclic imides to diols and amines, Green Chem. 22 (2020) 3079–3082, https://doi.org/10.1039/D0GC00570C.

[27] D.M. Sharma, B. Punji, 3d Transition metal-catalyzed hydrogenation of nitriles and alkynes, Chem. Asian J. 15 (2020) 690–708, https://doi.org/10.1002/asia.201901762.

[28] K. Sarkar, K. Das, A. Kundu, D. Adhikari, B. Maji, Phosphine-free manganese catalyst enables selective transfer hydrogenation of nitriles to primary and secondary amines using ammonia-borane, ACS Catal 11 (2021) 2786–2794, https://doi.org/10.1021/acscatal.0c05406.

[29] Y. Wang, L. Zhu, Z. Shao, G. Li, Y. Lan, Q. Liu, Unmasking the ligand effect in manganese-catalyzed hydrogenation: mechanistic insight and catalytic application, J. Am. Chem. Soc. 141 (2019) 17337–17349, https://doi.org/10.1021/jacs.9b09038.

[30] V. Papa, J. Fessler, F. Zaccaria, J. Hervochon, P. Dam, C. Kubis, A. Spannenberg, Z. Wei, H. Jiao, C. Zuccaccia, A. Macchioni, K. Junge, M. Beller, Efficient hydrogenation of N-heterocycles catalyzed by NNP–Manganese(I) pincer complexes at ambient temperature, Chem. Eur. J. 29 (2023) e202202774, https://doi.org/10.1002/chem.202202774.

[31] Z. Liu, Y.-J. Yu, G.-W. Wang, S.-M. Lu, Y.-G. Zhou, M.-W. Chen, Manganese-catalyzed asymmetric hydrogenation of multi-nitrogen heteroaromatic compounds, Org. Lett. 27 (2025) 9890–9895, https://doi.org/10.1021/acs.orglett.5c02777.

[32] A. Kumar, T. Janes, N.A. Espinosa-Jalapa, D. Milstein, Manganese catalyzed hydrogenation of organic carbonates to methanol and alcohols, Angew. Chem. Int. Ed. 57 (2018) 12076–12080, https://doi.org/10.1002/anie.201806289.

[33] X. Liu, T. Werner, Indirect reduction of CO2 and recycling of polymers by manganese-catalyzed transfer hydrogenation of amides, carbamates, urea derivatives, and polyurethanes, Chem. Sci. 12 (2021) 10590–10597, https://doi.org/10.1039/D1SC02663A.

[34] V. Zubar, Y. Lebedev, L.M. Azofra, L. Cavallo, O. El-Sepelgy, M. Rueping, Hydrogenation of CO_2-derived carbonates and polycarbonates to methanol and diols by metal–Ligand Cooperative Manganese catalysis, Angew. Chem. Int. Ed. 57 (2018) 13439–13443, https://doi.org/10.1002/anie.201805630.

[35] M.A. Stevens, A.L. Colebatch, Cooperative approaches in catalytic hydrogenation and dehydrogenation, Chem. Soc. Rev. 51 (2022) 1881–1898, https://doi.org/10.1039/D1CS01171E.

[36] J.R. Khusnutdinova, D. Milstein, Metal–Ligand cooperation, Angew. Chem. Int. Ed. 54 (2015) 12236–12273, https://doi.org/10.1002/anie.201503873.

[37] R. Noyori, S. Hashiguchi, Asymmetric transfer hydrogenation catalyzed by chiral ruthenium complexes, Acc. Chem. Res. 30 (1997) 97–102, https://doi.org/10.1021/ar9502341.

[38] R. Noyori, T. Okhuma, Asymmetric catalysis by architectural and functional molecular engineering: practical chemo- and stereoselective hydrogenation of ketones, Angew. Chem. Int. Ed. (40) (2001) 40–73, https://doi.org/10.1002/1521-3773(20010105)40:1<40::AID-−ANIE40>3.0.CO;2-5.

[39] R. Noyori, M. Koizumi, D. Ishii, T. Ohkuma, Asymmetric hydrogenation via architectural and functional molecular engineering, Pure Appl. Chem. 73 (2001) 227–232, https://doi.org/10.1351/pac200173020227.

[40] S. Weber, K. Kirchner, The role of metal-Ligand cooperation in Manganese(I)-catalyzed hydrogenation/dehydrogenation reactions, Eds, in: G. van Koten, K. Kirchner, M.E. Moret (Eds.), Metal-Ligand Co-operativity. Topics in Organometallic Chemistry, Metal-Ligand Co-operativity. Topics in Organometallic Chemistry, 68, Springer, Cham, 2020, https://doi.org/10.1007/3418_2020_66.

[41] K.Z. Demmans, M.E. Olson, R.H. Morris, Asymmetric transfer hydrogenation of ketones with well-defined Manganese(I) PNN and PNNP complexes, Organometallics 37 (2018) 4608–4618, https://doi.org/10.1021/acs.organomet.8b00625.

[42] Z. Császár, R. Kovács, M. Fonyó, J. Simon, A.C. Bényei, G. Lendvay, J. Bakos, G. Farkas, Testing the role of the backbone length using bidentate and tridentate ligands in manganese-catalyzed asymmetric hydrogenation, Mol. Catal. 529 (2022) 112531, https://doi.org/10.1016/j.mcat.2022.112531.

[43] L. Zeng, H. Yang, M. Zhao, J. Wen, J.H.R. Tucker, X. Zhang, *C1*-Symmetric PNP ligands for manganese-catalyzed enantioselective hydrogenation of ketones: reaction scope and enantioinduction mode, ACS Catal. 10 (2020) 13794–13799, https://doi.org/10.1021/acscatal.0c04206.

[44] A. Maji, S. Gupta, D. Panja, S. Sutradhar, S. Kundu, Hydrogenation of *N*-heterocycles by a well-defined phosphine-free manganese catalyst using Ammonia borane, Organometallics 42 (2023) 3385–3396, https://doi.org/10.1021/acs.organomet.3c00368.

[45] W. Yang, I. Yu Chernyshov, R.K.A. van Schendel, M. Weber, C. Müller, G. A. Filonenko, E.A. Pidko, Robust and efficient hydrogenation of carbonyl compounds catalysed by mixed donor Mn(I) pincer complexes, Nat. Commun. 12 (2021) 12, https://doi.org/10.1038/s41467-020-20168-2.

[46] R. van Putten, J. Benschop, V.J. de Munck, M. Weber, C. Müller, G.A. Filonenko, E. A. Pidko, Efficient and practical transfer hydrogenation of ketones catalyzed by a simple bidentate Mn−NHC complex, ChemCatChem 11 (2019) 5232–5235, https://doi.org/10.1002/cctc.201900882.

[47] M.B. Widegren, M.L. Clarke, Towards practical earth abundant reduction catalysis: design of improved catalysts for manganese catalysed hydrogenation, Catal. Sci. Technol. 9 (2019) 6047–6058, https://doi.org/10.1039/C9CY01601E.

[48] C.L. Oates, A.S. Goodfellow, M. Bühl, M.L. Clarke, Rational design of a facially coordinating P,N,N Ligand for Manganese-catalysed enantioselective hydrogenation of cyclic ketones, Angew. Chem. Int. Ed. 62 (2023) e202212479, https://doi.org/10.1002/anie.202212479.

[49] A.M. Krieger, V. Sinha, A.V. Kalikadien, E.A. Pidko, Metal-ligand cooparative activation of HX (X = H, Br, OR) bond on Mn based pincer complexes, Z. Anorg. Allg. Chem. 647 (2021) 1486–1494, https://doi.org/10.1002/zaac.202100078.

[50] H.-Y.T. Chen, D.D. Tommaso, G. Hogarth, C.R.A. Catlow, The effects of ligand variation on enantioselective hydrogenation catalysed by RuH_2(diphosphine)(diamine) complexes, Dalton Trans. 41 (2012) 1867–1877, https://doi.org/10.1039/c1dt11244a.

[51] W. Eschweiler, Ersatz von an stickstoff gebundenen Wasserstoffatomen durch die methylgruppe mit hülfe von Formaldehyd, Ber. Dtsch. Chem. Ges. 38 (1905) 880–882, https://doi.org/10.1002/cber.190503801154.

[52] A. Zirakzadeh, S.R.M.M. de Aguiar, B. Stoeger, M. Widhalm, K. Kirchner, Enantioselective transfer hydrogenation of ketones catalyzed by a Manganese complex containing an unsimmetrical chiral PNP' Tidentate ligand, ChemCatChem 9 (2017) 1744–1748, https://doi.org/10.1002/cctc.201700042.

[53] N.A. Espinosa-Jalapa, A. Kumar, G. Leitus, Y. Diskin-Posner, D. Milstein, Synthesis of cyclic imides by acceptorless dehydrogenative coupling of diols and amines catalyzed by a Manganese pincer complex, J. Am. Chem. Soc. 139 (2017) 11722–11725, https://doi.org/10.1021/jacs.7b08341.

[54] D. Fu, Z. Wang, M. Liu, S. Liu, Y. Wang, C. Wei, Y. Ma, Q. Liu, G.A. Solan, W.-H. Sun, Dehydrogenation of primary alcohols to carboxylic acids in water catalyzed by PNHN-manganese(I) carbonyl complexes, J. Catal. 436 (2024) 115601, https://doi.org/10.1016/j.jcat.2024.115601.

[55] P. Crochet, J. Gimeno, S. García-Granda, J. Borge, Five- and six-coordinate ruthenium(II) complexes containing 2-$ph_2PC_6H_4CH{=}N^tBu$ and 2-$ph_2PC_6H_4CH_2NH^tBu$ as chelate ligands: synthesis, characterization, and catalytic activity in transfer hydrogenation of ketones, Organometallics 20 (2001) 4369–4377, https://doi.org/10.1021/om010443r.

[56] E.W. Dahl, N.K. Szymczak, Hydrogen bonds dictate the coordination geometry of copper: characterization of a square-planar copper(I) ComplexAngew, Chem 128 (2016) 3153–3157, https://doi.org/10.1002/ange.201511527.

[57] K.-J. Haack, S. Hashiguchi, A. Fujii, T. Ikariya, R. Noyori, The catalyst precursor, catalyst, and intermediate in the Ru^{II}-promoted asymmetric hydrogen transfer between alcohols and ketones, Angew. Chem. Int. Ed. 36 (1997) 285–288, https://doi.org/10.1002/anie.199702851.

[58] M.D. Fryzuk, C.D. Montgomery, S.J. Rettigs, Synthesis and reactivity of ruthenium amide-phosphine complexes. Facile conversion of a ruthenium amide to a ruthenium amine via dihydrogen activation and ortho metalation. X-ray structure of $RuCl(C_6H_4PPh_2)$ [$NH(SiMe_2CH_2PPh_2)$], Organometallics 10 (1991) 467–473, https://doi.org/10.1021/om00048a025.

[59] Z. Császár, G. Farkas, A. Bényei, G. Lendvay, I. Tóth, J. Bakos, Stereoselective coordination: a six-membered P,N-chelate tailored for asymmetric allylic alkylation, Dalton Trans. 44 (2015) 16352–16360, https://doi.org/10.1039/C5DT02750K.

[60] A. Bondi, van der Waals volumes and radii, J. Phys. Chem. 68 (1964) 441–451, https://doi.org/10.1021/j100785a001.

[61] L. Zeng, H. Yang, M. Zhao, J. Wen, J.H.R. Tucker, X. Zhang, C1-Symmetric PNP ligands for manganese-catalyzed enantioselective hydrogenation of ketones: reaction scope and enantioinduction model ACS Catal. 10 (2020), 13794−13799. https://doi.org/10.1021/acscatal.0c04206.

[62] P.A. Dub, J.C. Gordon, The role of the metal-bound N-H functionality in Noyori-type molecular catalysts, Nat. Rev. Chem. 2 (2018) 396–408, https://doi.org/10.1038/s41570-018-0049-z.

[63] L. Falivene, Z. Cao, A. Petta, L. Serra, A. Poater, R. Oliva, V. Scarano, L. Cavallo, Towards the online computer-aided design of catalytic pockets, Nat. Chem. 11 (2019) 872–879, https://doi.org/10.1038/s41557-019-0319-5.

[64] R. van Putten, G.A. Filolenko, A.G. de Castro, C. Liu, M. Weber, C. Müller, L. Lefort, E. Pidko, Mechanistic complexity of asymmetric transfer hydrogenation with simple Mn-diamine catalysts, Organometallics 38 (2019) 3187–3196, https://doi.org/10.1021/acs.organomet.9b00457.

[65] H. Dai, W. Li, J.A. Krause, H. Guan, Experimental evidence of syn H−N−Fe−H configurational requirement for iron-based bifunctional hydrogenation catalysts, Inorg. Chem. 60 (2021) 6521–6535, https://doi.org/10.1021/acs.inorgchem.1c00328.

[66] E.S. Gulyaeva, R. Buhaibeh, M. Boundor, K. Azouzi, J. Willot, S. Bastin, C. Duhayon, N. Lugan, O.A. Filippov, J.B. Sortais, D.A. Valyaev, Y. Canac, Impact of the methylene bridge substitution in chelating NHC-phosphine Mn(I) catalyst for ketone hydrogenation, Chem. Eur. J. 30 (2024) e202304201, https://doi.org/10.1002/chem.202304201.

[67] Y. Zhang, B. Li, T. Wang, N. Duan, J. Zheng, H. Li, F. Zhang, X. Fang, Efficient hydrogenation of ketones over the diaminophosphino manganese complex, Dalton. Trans. 53 (2024) 16475–16479, https://doi.org/10.1039/D4DT02297A.